



Surface modification of silica gel for adsorptive removal of Ni²⁺ and Cd²⁺ from water

Atul Kumar Kushwaha^{a,b,*}, M.C. Chattopadhyaya^b

^aDepartment of Chemistry, Sri Sai University, Palampur, H.P., India

^bDepartment of Chemistry, University of Allahabad, Allahabad, U.P. 211002, India

Tel. +91 0532 2462393; email: atulkk2008@gmail.com

Received 18 September 2013; Accepted 20 January 2014

ABSTRACT

In this study, surface of silica gel was functionalized with 1,2-ethylenediamine. The synthesized materials were characterized by Fourier transform infrared spectroscopy, scanning electron microscope, and elemental analysis. Batch adsorption studies were carried out to analyze the adsorption of nickel and cadmium ions from aqueous solutions. The factors influencing % adsorptive removal of Ni²⁺ and Cd²⁺ onto the silica gel and functionalized silica gel, such as initial pH value of the Ni²⁺ and Cd²⁺ ion solutions, adsorbent dose, initial Ni²⁺ and Cd²⁺ ion concentration, contact time, and temperature were investigated. Langmuir and Freundlich isotherm models were used to determine the isotherm parameters associated with the adsorption process. The monolayer adsorption capacity of ASG for Ni²⁺ and Cd²⁺ increased from 4.69 to 19.6 and 7.63 to 27 mg/g, respectively, after modification of activated silica gel (ASG) surface with 1,2-ethylenediamine. Kinetic data were analyzed considering pseudo-first-order and pseudo-second-order kinetic models. Adsorption of Ni²⁺ and Cd²⁺ on ASG followed pseudo-first-order, while on 1,2-ethylenediamine functionalized silica gel (SGAm) followed pseudo-second-order kinetics. Negative values of Gibb's free energy change (ΔG°) showed that the adsorptions were feasible and spontaneous, and negative values of enthalpy change (ΔH°) confirmed exothermic adsorptions.

Keywords: Adsorption; Equilibrium; Nickel; Cadmium; Silica gel

1. Introduction

Silica gel is an amorphous inorganic polymer composed of internal siloxane and silanol groups distributed on the surface. Silica gel is chosen as a material for immobilization of organic compounds mainly due to its good mechanical strength, large specific surface area swelling stability, good thermal resistant properties, and fast metal-exchange kinetics. In recent years, much attention has been paid to the

chemical modifications of the surface of silica gel with various functional groups to improve its physical and chemical properties. Chemically modified silica gel finds useful applications as scavenger for toxic metal ions from contaminated water bodies. Pioneer work on the metal recovery using chemically modified silica gel has been carried out by a number of researchers. Bois et al. reported functionalized porous silica with aminopropyl (H₂N(CH₂)₃-), [amino-ethylamino]propyl (H₂N-(CH₂)₂-NH(CH₂)₃-), (2-aminoethylamino)-ethylamino]propyl (H₂N-(CH₂)₂-NH-(CH₂)₂-NH(CH₂)₃-),

*Corresponding author.

and mercaptopropyl (HS-(CH₂)₃-) groups for heavy metal ions adsorption [1]. Quintanilla et al. reported 2-mercaptothiazoline modified mesoporous silica for mercury removal from aqueous media [2]. Muresanu et al. reported modified SBA-15 mesoporous silica for heavy metal ions remediation [3]. Dey et al. reported attachment of linear poly(amido amine) to silica surface and evaluation of metal-binding behavior [4]. Repo et al. reported removal of Co(II) and Ni(II) ions from contaminated water using silica gel functionalized with EDTA and/or DTPA as chelating agents [5]. Benhamou et al. reported aqueous heavy metals removal on amine-functionalized Si-MCM-41 and Si-MCM-48 [6]. Ramadan et al. reported mercury removal from aqueous solutions using silica, polyacrylamide, and hybrid silica polyacrylamide aerogels [7]. Standeker et al. reported silica aerogels modified with mercapto functional groups used for Cu(II) and Hg(II) removal from aqueous solutions [8]. Jeong et al. reported removal of Cu(II) from water by tetrakis(4-carboxyphenyl) porphyrin-functionalized mesoporous silica [9]. In previously reported studies, trimethoxysilane derivatives were used as a means of attaching organic functional moieties on silica surfaces. Such derivatization however, means an additional step at an additional cost.

In present study, an alternative, economical approach has been tried to functionalize silica surface. The surface of activated silica gel (ASG) was functionalized with 1,2-ethylenediamine using coupling reaction and was tested for the removal of Ni²⁺ and Cd²⁺ from aqueous solutions by batch adsorption method.

2. Materials and methods

2.1. Synthesis of ASG and SGAm

Silica gel G (SG) was obtained from Sigma Aldrich Chemicals Pvt. Ltd., India. Activation of SG was done by adding 100 mL of 6 M HCl in 20 g of SG and the mixture was allowed to reflux with continuous stirring for 4 h. The resultant material was filtered, washed with double-distilled water until the pH became 7, and dried at 150 °C for 5 h. The resulting material, ASG was kept in a desiccator for its use as an adsorbent.

2.5 mM of SOCl₂ (Merck) was added to ASG (2.5 mM) and kept on reflux for 2 h at 80–90 °C. The mixture was poured into crushed ice, stirred for 5 min, and the resulting solid (ASG-Cl) was filtered, washed well with toluene, and dried. *t*-BuOK

(2.5 mM) and *n*-Bu₄NBr (0.1 mM) were added to a cooled solution (0 °C) of 1,2-ethylenediamine (2.0 mM) in DMF (5 mL) and the resulting reaction mixture was stirred at 0 °C for 15 min. After that a solution of ASG-Cl (2.0 mM) in THF was added and the resulting reaction mixture was left for stirring (24 h) at room temperature. The resulting reaction mixture was filtered, washed with double-distilled water, and dried at 100 °C. Dried material and silica gel amine derivative of 1,2-ethylenediamine (SGAm) were kept in desiccators for using as adsorbents.

2.2. Adsorption experiments

Batch adsorption experiments were carried out to determine the effects of pH, adsorbent dose, initial metal ion concentration, contact time, and temperature by varying the parameters under study and keeping other parameters constant. Stock solution (1,000 mg/L) of metal ion was prepared by dissolving requisite amount of Ni (NO₃)₂·6H₂O (Merck) and Cd (NO₃)₂·4H₂O (Merck) into double-distilled water. It was subsequently diluted to different concentrations (5, 10, 15, 20, and 25 mg L⁻¹) and the pH of metal ion solutions were maintained by adding 0.1 M HNO₃ or 0.1 M NaOH. In each experiment pre-weighed amounts of adsorbents were added to 50 mL of metal ion solution in 150 mL conical flasks and stirred with a magnetic stirrer (Remi) at the speed of 200 rpm. The adsorption was monitored by determining the concentration of metal ion in solution by atomic absorption spectrophotometer (ECIL 4141).

Percentage removal of metal ion and quantity of metal ion adsorbed on adsorbent at the time of equilibrium (q_e) was calculated using Eq. (1) and (2), respectively.

$$\% \text{ Removal} = 100 \times (C_0 - C_e) / C_0 \quad (1)$$

$$q_e = (C_0 - C_e) V / M \quad (2)$$

where C_0 and C_e are the initial and the equilibrium concentrations (mg/L) of metal ion in solution, respectively. q_e is quantity of metal ion adsorbed on the adsorbent at the time of equilibrium (mg/g), V is volume (L) of solution, and M is mass of adsorbent (g) taken for the experiment.

3. Results and discussion

3.1. Characterization of ASG and SGAm

The Fourier transform infrared (FTIR) spectra of ASG and SGAm were recorded on FTLA2000 spectrophotometer using KBr disk method in the range of 4,000–500 cm^{-1} (Fig. 1). FTIR spectrum of ASG showed a band at 1,027 cm^{-1} due to asymmetric stretching of Si–O–Si and corresponding symmetric stretching was observed at 805 cm^{-1} . The Si–O–Si bending mode was positioned at 502 cm^{-1} . The peaks at 3,473 and 1,594 cm^{-1} were due to the stretching and bending of O–H groups present in silica, respectively. FTIR spectrum of SGAm showed the same bands as was observed in ASG with some new peaks. A peak at 1,684 cm^{-1} was due to bending vibration of N–H groups. Bands at 1,416 and 1,315 were due to the bending vibrations of C–H groups. The bands of N–H and C–H groups which had come from 4,4'-diaminodiphenylmethane confirmed the formation of SGAm.

SEM micrographs (Fig. 2(a) and (b)) revealed the surface morphologies of the ASG and SGAm, respectively, which were investigated by SEM (SUPRA 40VP) operated at 10 kV accelerating voltage. The surfaces of ASG and SGAm were homogenous, porous, and rough in nature. The changes in surface morphology of ASG were clearly seen after its functionalization. Elemental analysis of ASG and SGAm was done by Elementar Vario EL III and the wt.% of C in ASG and SGAm was found to be 0.3 and 5.28%, respectively and the wt.% of N in SGAm was 6.25%.

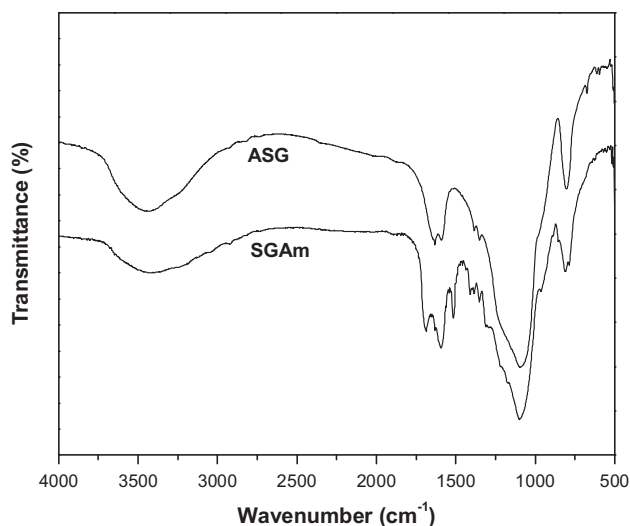


Fig. 1. FTIR spectra of ASG and SGAm.

3.2. Effect of pH

The pH of aqueous solution has a significant effect on the adsorptive uptake of metal ions presumably due to its impact on both the surface binding-sites of the adsorbent and the presence of hydrogen ions in solution. The influence of pH on removal of metal ions was studied over the pH of range 2–6. Fig. 3 showed that the % removal of metal ions increased as pH increased from 2 to 6. At lower pH values, the hydrogen ion concentration in solution increased, which resulted in competition with metal ions for binding sites of the adsorbent and reduced the adsorbed amounts of metal ions. At higher pH values, the presence of hydrogen ions in solution decreased, and the adsorbent surface also deprotonated, increasing the adsorption of metal ion [10]. Further increase in pH causes precipitation of metal ions due to formation of hydroxide, therefore, the pH higher than 6 were avoided and all subsequent studies were carried out at pH 6.

3.3. Effect of adsorbent dose

The effect of adsorbent dose on removal was studied in the range of 0.5–3 g/L. Fig. 4 showed that the % removal increased from 5 to 19%, 12 to 35%, 21 to 60%, and 41 to 92% for ASG-Ni, ASG-Cd, SGAm-Ni, and SGAm-Cd systems, respectively, as adsorbent dose increased from 0.5 to 2 g/L. This increase in % removal was due to an increase in the adsorptive surface area and the availability of more active adsorption sites [11]. Further increase in the adsorbent dose did not cause any significant change because equilibrium was achieved between solid and solution phase. Therefore, 2 g/L adsorbent dose was chosen for successive experiments.

3.4. Effect of contact time

Fig. 5 showed the effect of contact time on removal of metal ions from aqueous solution. It can be seen that the rate of adsorption of metal ions was very rapid in the first 5 min, thereafter it declined slowly with lapse of time. Maximum % adsorption was found at 30 min of contact time, and thereafter no change was observed. This indicates that the adsorption process reached the equilibrium [12].

3.5. Effect of initial metal ion concentration

To study the effect of initial metal ion concentration on removal, the experiments were conducted over the range of initial metal ion concentrations (5–25 mg/L).

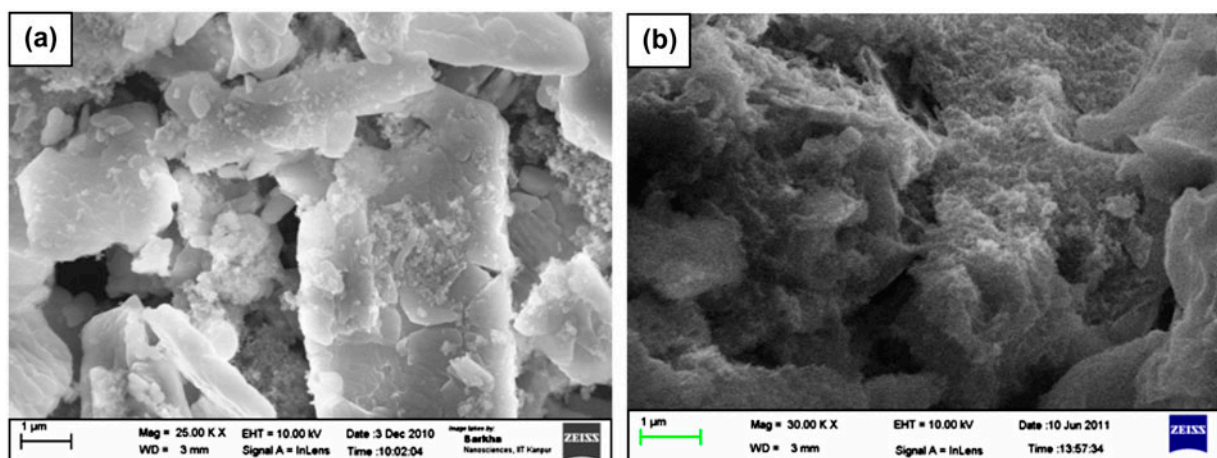


Fig. 2. SEM images of ASG (a) and SGAm (b).

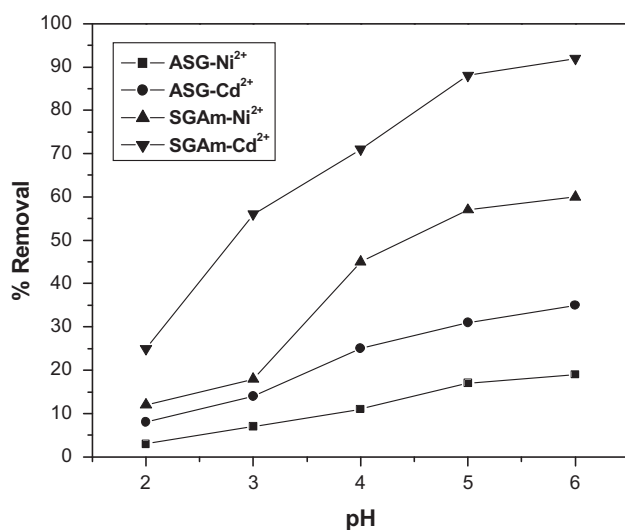


Fig. 3. Effect of pH on the removal of Ni²⁺ and Cd²⁺ by ASG and SGAm.

The % removal of metal ions decreased from 19 to 11%, 35 to 20%, 60 to 44%, and 92 to 79% for ASG-Ni, ASG-Cd, SGAm-Ni, and SGAm-Cd systems, respectively, as initial metal ion concentration increased from 5 to 25 mg/L. The decrease in % removal of metal ion was due to lesser availability of adsorption sites [13].

3.6. Adsorption kinetics

Several kinetic models have been proposed to clarify the mechanism of solute adsorption from aqueous solution onto an adsorbent.

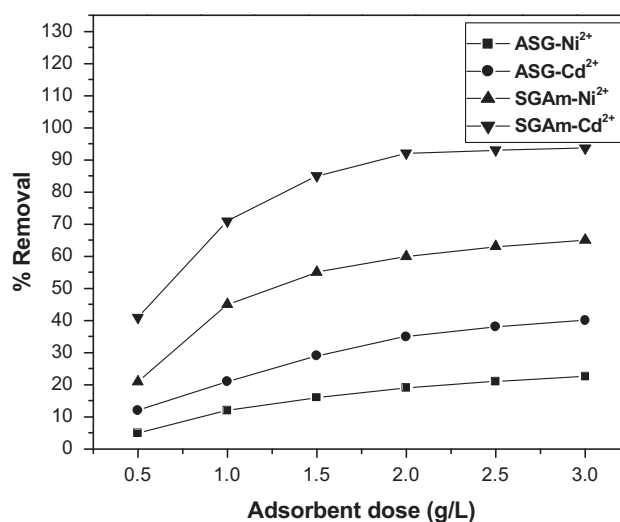


Fig. 4. Effect of adsorbent dose on the removal of Ni²⁺ and Cd²⁺ by ASG and SGAm.

The rate constant of adsorption was determined from the pseudo-first-order rate expression (Eq. (3)) given by Lagergren [14]:

$$\ln(q_e - q_t) = \ln q_e - k_1 t \quad (3)$$

where q_e and q_t are the amounts of metal ions adsorbed at equilibrium and at time t (mg/g), respectively, and k_1 (min^{-1}) is rate constant of adsorption. The values of k_1 and $q_{e,\text{cal}}$ were calculated from the slopes ($-k_1$) and intercepts ($\ln q_e$) of the plots of $\ln(q_e - q_t)$ vs. t (Fig. 6), respectively, and are presented in Table 1.

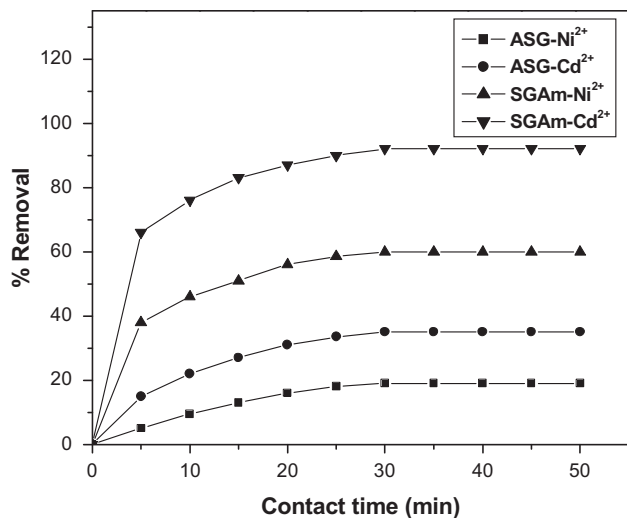


Fig. 5. Effect of contact time on the removal of Ni^{2+} and Cd^{2+} by ASG and SGAm.

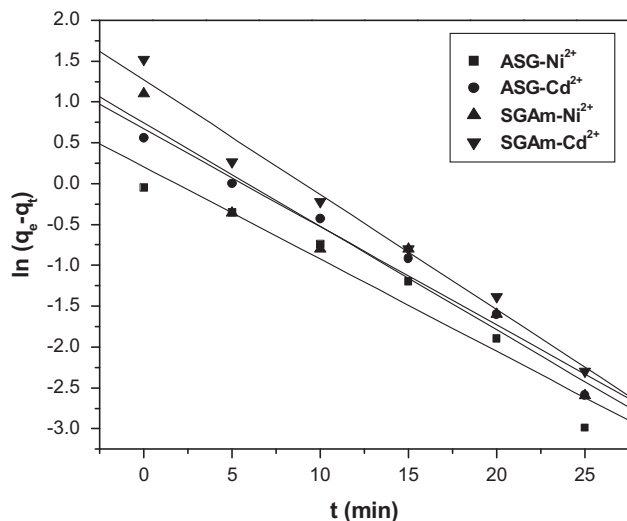


Fig. 6. Pseudo-first-order kinetic plots for the adsorption of Ni^{2+} and Cd^{2+} on ASG and SGAm.

Results showed a good agreement between experimental and calculated q_e values for adsorption of Ni^{2+} and Cd^{2+} onto ASG. The correlation coefficients for the pseudo-first-order kinetic model for ASG were 0.941 and 0.975 for Ni^{2+} and Cd^{2+} , respectively, which indicates the applicability of the pseudo-first-order equation for the adsorption of Ni^{2+} and Cd^{2+} onto ASG. Although the correlation coefficient value for adsorption of metal ions onto SGAm was high, the experimental q_e values did not agree with the calculated ones, obtained from the

linear plots. This showed that the adsorption of metal ions onto SGAm did not follow pseudo-first-order kinetics.

The pseudo-second-order adsorption kinetics [15] may be written as follows:

$$t/q_t = 1/k_2q_e^2 + t/q_e \quad (4)$$

where k_2 is the rate constant of adsorption (g/mg min), q_e and q_t are the amounts of metal ions adsorbed at equilibrium and at time t (mg/g), respectively. The values of k_2 and $q_{e,\text{cal}}$ were calculated from the intercepts ($1/k_2q_e^2$) and slopes ($1/q_e$) of the plots of t/q_t vs. t . (Fig. 7), respectively, and are presented in Table 1. Results showed that the correlation coefficient of adsorption of Ni^{2+} and Cd^{2+} onto SGAm for the pseudo-second-order kinetic model was 0.985 and 0.993, respectively, and a good agreement between experimental and calculated q_e values indicated the applicability of pseudo-second-order kinetic model for the adsorption of Ni^{2+} and Cd^{2+} on SGAm.

3.7. Adsorption isotherms

The analysis of equilibrium data to construct adsorption isotherms is usually important for design of adsorption systems. Adsorption isotherms express the mathematical relationships between the quantity of adsorbate and equilibrium concentration of adsorbate remaining in the solution at a constant temperature. In the present study the equilibrium data were analyzed using the Langmuir and Freundlich isotherm models.

3.7.1. Langmuir isotherm model

The Langmuir model is valid for monolayer adsorption onto a surface with a finite number of identical sites which are homogeneously distributed over the adsorbent surfaces.

The saturated monolayer isotherm can be represented as:

$$q_e = Q_m b C_e / (1 + b C_e) \quad (5)$$

The linearized forms of Eq. (5) can be written as follows [16]:

$$C_e/q_e = 1/bQ_m + C_e/Q_m \quad (6)$$

where q_e is the adsorption density (mg/g) at equilibrium of metal ion, C_e is the equilibrium concentration

Table 1
Kinetic parameters for the adsorption of Ni²⁺ and Cd²⁺ on ASG and SGAm

Adsorption systems	$q_{e,exp}$	Pseudo-first-order			Pseudo-second-order		
		$q_{e,cal}$	K_1	R^2	$q_{e,cal}$	K_2	R^2
ASG-Ni ²⁺	0.9	0.95	0.113	0.941	1.22	0.029	0.752
ASG-Cd ²⁺	1.7	1.74	0.120	0.975	1.95	0.102	0.936
SGAm-Ni ²⁺	3.0	2.10	0.126	0.920	3.13	0.140	0.985
SGAm-Cd ²⁺	4.6	3.56	0.140	0.978	4.73	0.141	0.993

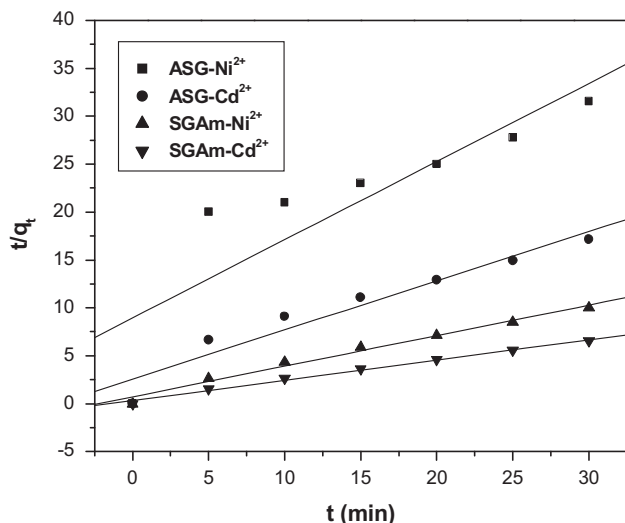


Fig. 7. Pseudo-second-order kinetic plots for the adsorption of Ni²⁺ and Cd²⁺ on ASG and SGAm.

(mg/L) of the metal ion in solution, Q_m is the monolayer adsorption capacity (mg/g) and b is the Langmuir constant (L/mg) related to the free energy of adsorption. The values of Q_m and b were calculated from the slopes ($1/Q_m$) and intercepts ($1/bQ_m$) of the linear plots of C_e/q_e vs. C_e (Fig. 8), and are given in Table 2. Linear plots of C_e/q_e vs. C_e showed that the adsorption followed the Langmuir isotherm model for all the four systems. Experimental results showed that the monolayer adsorption capacity of adsorbents for metal ions for all the four systems was in the order ASG-Ni²⁺ < ASG-Cd²⁺ < SGAm-Ni²⁺ < SGAm-Cd²⁺.

3.7.2. Freundlich isotherm model

The empirical Freundlich isotherm model is based on adsorption on a heterogeneous surface and can be expressed by the following equation [17]:

$$q_e = K_f C_e^{1/n} \quad (7)$$

The logarithmic forms of Eq. (7) can be written as follows:

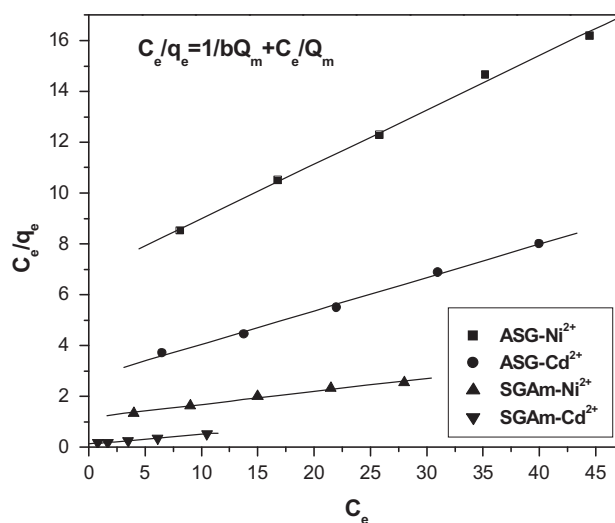


Fig. 8. Langmuir isotherm plots for the adsorption of Ni²⁺ and Cd²⁺ on ASG and SGAm.

$$\ln q_e = \ln K_f + (1/n) \ln C_e \quad (8)$$

where K_f and n are Freundlich constants related to adsorption capacity [$\text{mg g}^{-1} (\text{mg L}^{-1})^{-1/n}$] and adsorption intensity of adsorbents, respectively. The values of the K_f and n were calculated from the intercepts ($\ln K_f$) and slopes ($1/n$) of the plots $\ln q_e$ vs. $\ln C_e$ (Fig. 9), and are presented in Table 2. Linear plots of $\ln q_e$ vs. $\ln C_e$ showed that the adsorption isotherm for all the four systems also fitted well in the Freundlich isotherm model and the adsorption capacity (K_f) of adsorbents for metal ion was increased in the order ASG-Ni²⁺ < ASG-Cd²⁺ < SGAm-Ni²⁺ < SGAm-Cd²⁺. The values of $n > 1$ indicated favorable adsorption conditions [18,19].

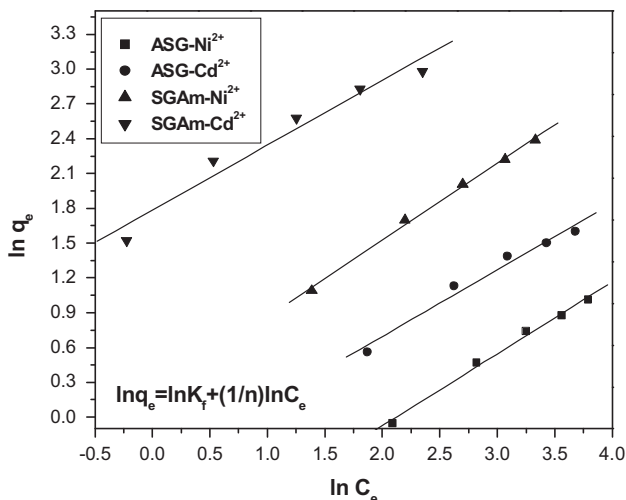
3.8. Adsorption thermodynamics

To observe the effect of temperature on removal of Ni²⁺ and Cd²⁺ onto ASG and SGAm, experiments were conducted at three different temperatures 303,

Table 2

Isotherm parameters for the adsorption of Ni²⁺ and Cd²⁺ on ASG and SGAm

Adsorption systems	Langmuir isotherm parameters			Freundlich isotherm parameters		
	Q_{\max}	b	R^2	K_f	n	R^2
ASG-Ni ²⁺	4.69	0.031	0.996	0.26	1.61	0.993
ASG-Cd ²⁺	7.63	0.047	0.996	0.63	1.74	0.974
SGAm-Ni ²⁺	19.6	0.043	0.987	1.22	1.50	0.996
SGAm-Cd ²⁺	27.0	0.28	0.996	5.95	1.78	0.955

Fig. 9. Freundlich isotherm plots for the adsorption of Ni²⁺ and Cd²⁺ on ASG and SGAm.

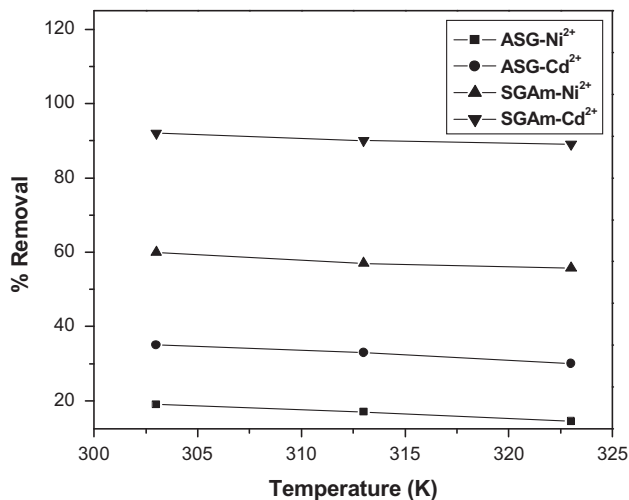
313, and 323 K. From Fig. 10, it can be observed that the adsorption decreased as temperature increased, which indicates that low temperature favors metal ion adsorption for all the four systems. This may be due to a tendency for the metal ion to escape from the solid phase to the bulk phase with an increase in temperature of the solution. A similar observation was also reported in the study on the adsorption of metals on modified and unmodified kaolinite clay [20].

Thermodynamic parameters such as enthalpy (ΔH°), entropy (ΔS°), and Gibb's free energy (ΔG°) are important for better understanding of the effect of temperature on adsorption, which were determined by Eq. (9) [21] and (10).

$$\ln (q_e m / C_e) = \Delta S^\circ / R - \Delta H^\circ / RT \quad (9)$$

$$\Delta G^\circ = \Delta H^\circ - T \Delta S^\circ \quad (10)$$

where m is the adsorbent dose (g/L), C_e is the equilibrium concentration (mg/L) of the metal ion in solution

Fig. 10. Effect of temperature on the removal of Ni²⁺ and Cd²⁺ by ASG and SGAm.

and $q_e m$ is the solid-phase concentration (mg/L) at equilibrium. R is the gas constant (8.314 J/mol/K), and T is the temperature (K). ΔH° , ΔS° , and ΔG° are changes in enthalpy (J/mol), entropy (J/mol/K), and Gibb's free energy (J/mol), respectively.

The values of ΔH° and ΔS° were determined from the slope ($-\Delta H^\circ / R$) and the intercept ($\Delta S^\circ / R$) of the plots of $\ln (q_e m / C_e)$ vs. $1/T$. The ΔG° values were calculated by using Eq. (10). The values of thermodynamic parameters are presented in Table 3. Negative values of ΔG° for the adsorption of Ni²⁺ and Cd²⁺ on SGAm at all three temperatures indicated that the adsorption process was feasible and spontaneous in nature. The ΔG° value was slightly positive for the adsorption of Ni²⁺ and Cd²⁺ on ASG and showed lower affinity of ASG for Ni²⁺ and Cd²⁺. Negative values of ΔH° suggested the adsorption process was exothermic in nature. Negative value of ΔS° described the decrease in randomness at the adsorbent-solution interface during the adsorption.

Table 3

Thermodynamic parameters for the adsorption of Ni²⁺ and Cd²⁺ on ASG and SGAm

Adsorption systems	ΔH° (kJ/mol)	ΔS° (J/mol/K)	ΔG° (kJ/mol)		
			303 K	313 K	323 K
ASG-Ni ²⁺	-12.62	-53.54	3.601	4.136	4.672
ASG-Cd ²⁺	-9.02	-34.83	1.524	1.872	2.221
SGAm-Ni ²⁺	-7.04	-19.95	-1.001	-0.802	-0.602
SGAm-Cd ²⁺	-13.94	-25.86	-6.104	-5.845	-5.587

4. Conclusions

The % removal of Ni²⁺ and Cd²⁺ increased from 19 to 60% and 35 to 92%, respectively, after modification of ASG surface with 1,2-ethylenediamine. The optimum condition for the adsorption was found to be pH 6, at temperature 303 K and 2 g/L of adsorbent dose. Adsorption of Ni²⁺ and Cd²⁺ on ASG followed pseudo-first-order kinetic model and adsorption of Ni²⁺ and Cd²⁺ on SGAm followed pseudo-second-order kinetic model. Equilibrium studies showed that the adsorption of metal ions onto ASG and SGAm followed the Langmuir and Freundlich isotherm models. The monolayer adsorption capacity was found to be 4.69, 7.63, 19.6, and 27 mg/g for ASG-Ni²⁺, ASG-Cd²⁺, SGAm-Ni²⁺, and SGAm-Cd²⁺ systems, respectively. Negative values of ΔG° for the adsorption of Ni²⁺ and Cd²⁺ on SGAm at all three temperatures indicated that the adsorption process was feasible and spontaneous in nature. The ΔG° value was slightly positive for the adsorption of Ni²⁺ and Cd²⁺ onto ASG and showed lower affinity for ASG for Ni²⁺ and Cd²⁺. Negative values of ΔH° suggested the adsorption process was exothermic in nature. Negative value of ΔS° described the decrease in randomness at the adsorbent–solution interface during the adsorption.

Acknowledgements

Authors are thankful to the SAIF-CDRI, Lucknow, for elemental analysis, Dr Dinesh Deva of Nanoscience, IIT Kanpur, for recording SEM, and the Council of Scientific and Industrial Research (CSIR), New Delhi, India, for the financial support.

References

- [1] L. Bois, A. Bonhomme, A. Ribes, B. Pais, G. Raffin, F. Tessier, Functionalized silica for heavy metal ions adsorption, *Colloids and Surfaces A: Physicochem. Eng. Aspects* 221 (2003) 221–230.
- [2] D. Pérez-Quintanilla, I. Hierro, M. Fajardo, I. Sierra, 2-Mercaptothiazoline modified mesoporous silica for mercury removal from aqueous media, *J. Hazard. Mater.* 134 (2006) 245–256.
- [3] M. Muresanu, A. Reiss, I. Stefanescu, E. David, V. Parvulescu, G. Renard, V. Hulea, Modified SBA-15 mesoporous silica for heavy metal ions remediation, *Chemosphere* 73 (2008) 1499–1504.
- [4] R.K. Dey, T. Patnaik, V.K. Singh, S.K. Swain, C. Airoidi, Attachment of linear poly(amido amine) to silica surface and evaluation of metal-binding behavior, *Appl. Surf. Sci.* 255 (2009) 8176–8182.
- [5] E. Repo, T.A. Kurniawan, J.K. Warchol, M.E.T. Sillanpää, Removal of Co(II) and Ni(II) ions from contaminated water using silica gel functionalized with EDTA and/or DTPA as chelating agents, *J. Hazard. Mater.* 171 (2009) 1071–1080.
- [6] A. Benhamou, M. Baudu, Z. Derriche, J.P. Basly, Aqueous heavy metals removal on amine-functionalized Si-MCM-41 and Si-MCM-48, *J. Hazard. Mater.* 171 (2009) 1001–1008.
- [7] H. Ramadan, A. Ghanem, H. El-Rassy, Mercury removal from aqueous solutions using silica, polyacrylamide and hybrid silica-polyacrylamide aerogels, *Chem. Eng. J.* 159 (2010) 107–115.
- [8] S. Štandeker, A. Veronovski, Z. Novak, Željko Knez, Silica aerogels modified with mercapto functional groups used for Cu(II) and Hg(II) removal from aqueous solutions, *Desalination* 269 (2011) 223–230.
- [9] E.Y. Jeong, M.B. Ansari, Y.H. Mo, S.E. Park, Removal of Cu(II) from water by tetrakis(4-carboxyphenyl) porphyrin-functionalized mesoporous silica, *J. Hazard. Mater.* 185 (2011) 1311–1317.
- [10] Z.A. Al-Anber, M.A.D. Matouq, Batch adsorption of cadmium ions from aqueous solution by means of olive cake, *J. Hazard. Mater.* 151 (2008) 194–201.
- [11] U. Garg, M.P. Kaur, G.K. Jawa, D. Sud, V.K. Garg, Removal of cadmium (II) from aqueous solutions by adsorption on agricultural waste biomass, *J. Hazard. Mater.* 154 (2008) 1149–1157.
- [12] V.C. Srivastava, I.D. Mall, I.M. Mishra, Equilibrium modelling of single and binary adsorption of cadmium and nickel onto bagasse fly ash, *Chem. Eng. J.* 117 (2006) 79–91.
- [13] N. Azouaou, Z. Sadaoui, A. Djaafri, H. Mokaddem, Adsorption of cadmium from aqueous solution onto untreated coffee grounds: Equilibrium, kinetics and thermodynamics, *J. Hazard. Mater.* 184 (2010) 126–134.
- [14] S. Lagergren, About the theory of so called adsorption of soluble substances, *Ksver Vetenskapsakad Handl.* 24 (1898) 1–6.

- [15] Y.S. Ho, G. McKay, Pseudo-second order model for sorption processes, *Process Biochem.* 34 (1999) 451–465.
- [16] H.K. Boparai, M. Joseph, D.M. O'Carroll, Kinetics and thermodynamics of cadmium ion removal by adsorption onto nano zerovalent iron particles, *J. Hazard. Mater.* 186 (2011) 458–465.
- [17] A. Fouladi Tajar, T. Kaghazchi, M. Soleimani, Adsorption of cadmium from aqueous solutions on sulfurized activated carbon prepared from nut shells, *J. Hazard. Mater.* 165 (2009) 1159–1164.
- [18] B.H. Hameed, D.K. Mahmoud, A.L. Ahmad, Equilibrium modeling and kinetic studies on the adsorption of basic dye by a low-cost adsorbent: Coconut (*Cocos nucifera*) bunch waste, *J. Hazard. Mater.* 158 (2008) 65–72.
- [19] B.H. Hameed, Grass waste: A novel sorbent for the removal of basic dye from aqueous solution, *J. Hazard. Mater.* 166 (2009) 233–238.
- [20] K.G. Bhattacharyya, S.S. Gupta, Adsorption of a few heavy metals on natural and modified kaolinite and montmorillonite: A review, *Adv. Colloid Interface Sci.* 140 (2008) 114–131.
- [21] B.K. Nandi, A. Goswami, M.K. Purkait, Adsorption characteristics of brilliant green dye on kaolin, *J. Hazard. Mater.* 161 (2009) 387–395.